Electronic Supplementary Information

Pt-carbon interactions-determined reaction pathway and selectivity for hydrogenation of 5-hydroxymethylfurfural over carbon supported Pt catalysts

Xiaofeng Wang,[a,*] Chengcheng Zhang,[a] Baitang Jin,[b] Xinhua Liang,[b] Qingfa Wang,[c] Zhe Zhao,[a] Qingbo Li[a]

[a] College of Environmental Science and Engineering, Dalian Maritime University, Dalian 116026, China

[b] Department of Chemical and Biochemical Engineering, Missouri University of Science and Technology, Rolla, MO 65409, United States

[c] Key Laboratory of Green Chemical Technology of Ministry of Education, School of Chemical Engineering and Technology, Tianjin University, Tianjin 300072, China

* Corresponding author, email: Xiaofeng Wang, wangxf@dlmu.edu.cn

Experimental details

Catalyst preparation by ALD. Platinum (Pt) nanoparticles (NPs) were deposited by ALD using (methylcyclopentadienyl)trimethyl platinum [(MeCp)PtMe$_3$] as the Pt precursor and oxygen (O$_2$) as the other reactant at 300 °C in a fluidized bed reactor (Figure S1), as described previously [1, 2]. In a typical run, 3 g of substrates were loaded into the reactor. Before the reaction, the substrates were degassed at 300 °C for 4 hr. During the ALD process, solid (MeCp)PtMe$_3$ (0.3 g) was heated and maintained at 70 °C, and carried by nitrogen (N$_2$) to enter the reactor. (MeCp)PtMe$_3$ and O$_2$ were fed separately into the reactor. The particle substrates were fully fluidized with a gas flow rate controlled by mass flow controllers. The reactor was also subjected to vibration via vibrators to improve the quality of particle fluidization during the ALD process [3]. N$_2$ was used as a flush

gas to remove unreacted precursors and any byproducts during the reaction. A typical Pt ALD cycle included the following steps: (MeCp)PtMe$_3$ dose (300 s), N$_2$ purge (600 s), evacuation (10 s); O$_2$ dose (600 s), N$_2$ purge (600 s), evacuation (10 s).

Ni ALD was carried out following the similar procedures using bis(cyclopentadienyl)nickel (NiCp$_2$) and hydrogen (H$_2$) as precursors at 300 °C. The solid NiCp$_2$ was loaded in a heated bubbler and carried by N$_2$. A typical Ni ALD cycle included the following steps: NiCp$_2$ dose (600 s), N$_2$ purge (900 s), evacuation (10 s); H$_2$ dose (900 s), N$_2$ purge (900 s), evacuation (10 s).

N$_2$ adsorption-desorption measurements. Nitrogen adsorption and desorption isotherms of substrates and catalysts were obtained at -196 ºC. The surface area and the total pore volume of the samples were calculated using the Brunauer-Emmett-Teller (BET) method in a relative pressure range of 0.05-0.25 and the adsorption quantity at a relative pressure of $P/P_0 = 0.99$, respectively. The pore size distributions were derived from the desorption branches of the isotherms using the Barrett-Joyner-Halenda (BJH) method.

High-resolution transmission electron microscopy (HRTEM). The supported Pt NPs were visualized with a FEI Tecnai F20 field emission gun high-resolution TEM. Samples were directly supported on holey-carbon Cu grids. At least 100 NPs on supports were measured to get an average Pt particle size. STEM and EDS analysis were used to verify the PtNi bimetallic nanoparticles.

X-ray powder diffraction (XRD). The crystal structure of Pt catalysts was detected by XRD with filtered Cu Ka radiation (λ= 1.5406 Å). The scanning range was 2θ from 10º to 90º, with a scanning rate of 0.025 º/s.

X-ray photoelectron spectroscopy (XPS). XPS spectra of Pt catalysts were recorded with a Kratos Axis 165 X-ray photoelectron spectrometer using a monochromatic Al Kα radiation (hv= 1486.6 eV), at a take-off angle of 0°. The survey scan spectra and Pt 4f core level spectra were recorded at a pass energy of 160 eV and 20 eV, respectively. The binding energy value was corrected by C 1s signal of 288.2 eV for the Pt/g-C$_3$N$_4$-IM catalyst, and that for all other catalysts were corrected by C 1s signal of 284.5 eV.

H₂ temperature programmed reduction (H₂-TPR) analysis. The reduction properties of the supported Pt catalysts were analyzed by H_2-TPR. The reaction temperature was programmed to rise at a heating rate of 10 ℃/min up to 800 ℃ and the flow rate was 20 mL/min of 10 mol% H_2/Ar gas. The consumption amount of H_2 during the H_2-TPR was analyzed and measured by a thermal conductivity detector (TCD, Micromeritics Autochem II 2920).
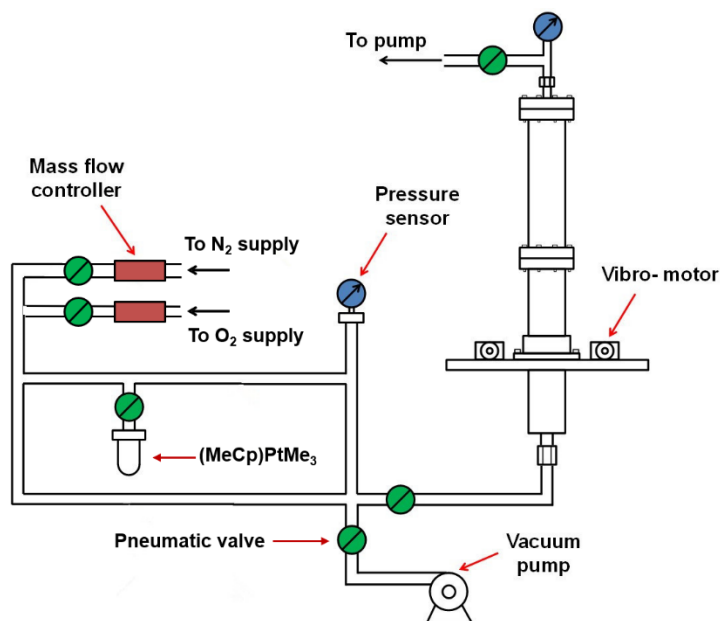

Figure S1. Scheme of atomic layer deposition reactor for Pt ALD.

(a)

(b)
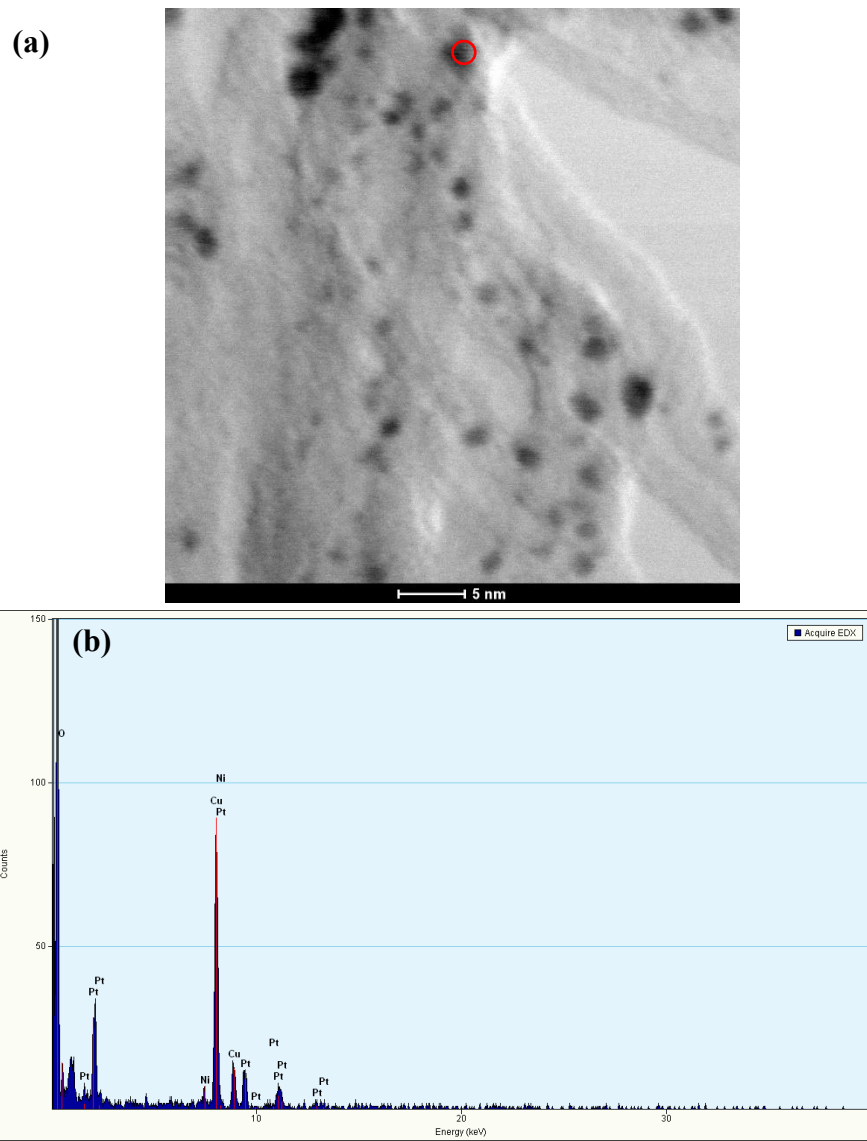
Figure S2. (a) STEM image of PtNi/CNTs-ALD and (b) EDS analysis of a selected nanoparticle (the labeled point).
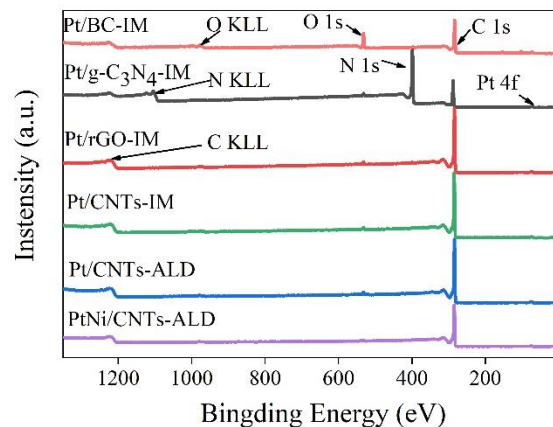
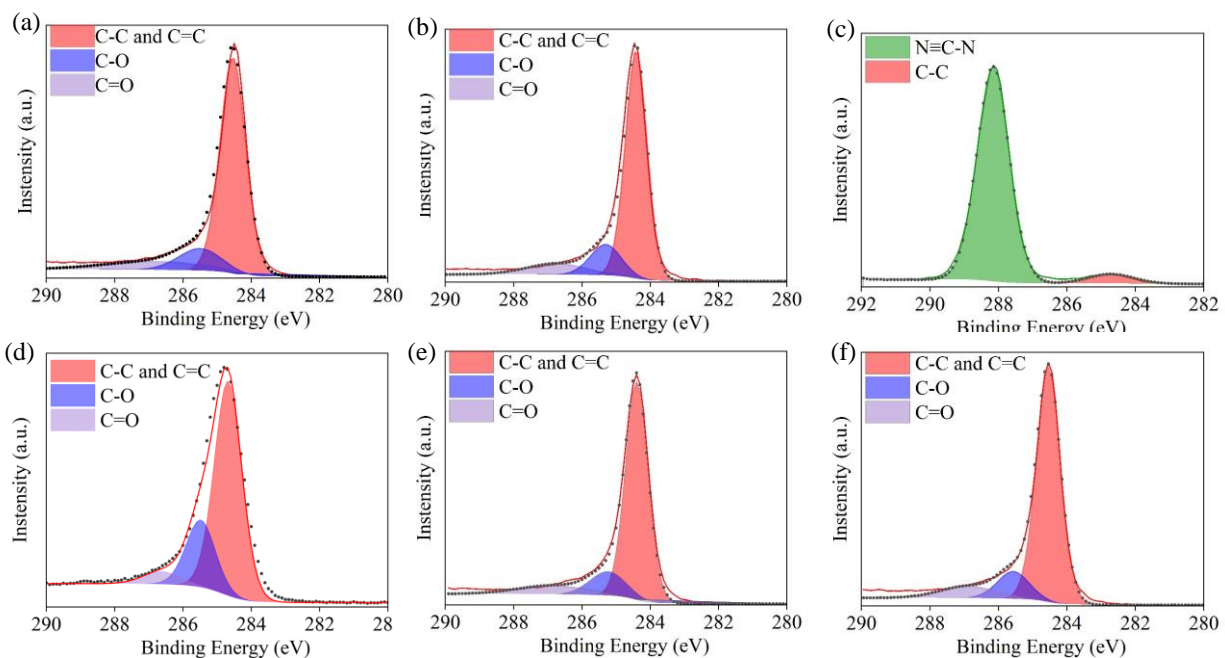**Figure S3.** XPS spectra of survey scan for the Pt-based catalysts.

Figure S4. XPS spectra of C 1s for different Pt catalysts: (a) Pt/CNTs-IM, (b) Pt/rGO-IM, (c) Pt/g-C_3N_4-IM, (d) Pt/BC-IM, (e) Pt/CNTs-ALD and (f) PtNi/CNTs-ALD.
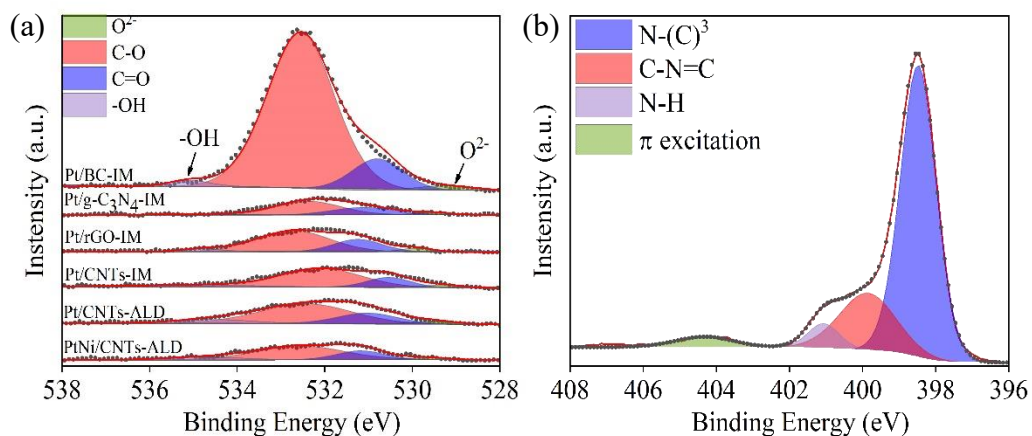
Figure S5. XPS spectra of (a) O 1s for the Pt/CNTs-IM, Pt/rGO-IM, Pt/g-C$_3$N$_4$-IM, Pt/BC-IM, Pt/CNTs-ALD and PtNi/CNTs-ALD catalysts and (b) N 1s for the Pt/g-C$_3$N$_4$ catalyst.

Table S1. Ratios of Pt species and oxygen groups analyzed by XPS.

	Pt^0/Pt^{II}	C-C&C=C/C=O/C-O
Pt/CNTs-IM	74/26	75/12/13
Pt/rGO-IM	73/27	75/10/15
Pt/g-C$_3$N$_4$-IM	76/24	93/7[a]
Pt/BC-IM	75/25	71/21/8
Pt/CNTs-ALD	79/21	78/12/10
PtNi/CNTs-ALD	71/29	76/14/10

[a] Ratio of N=C-N to C-C for the Pt/g-C$_3$N$_4$-IM catalyst.
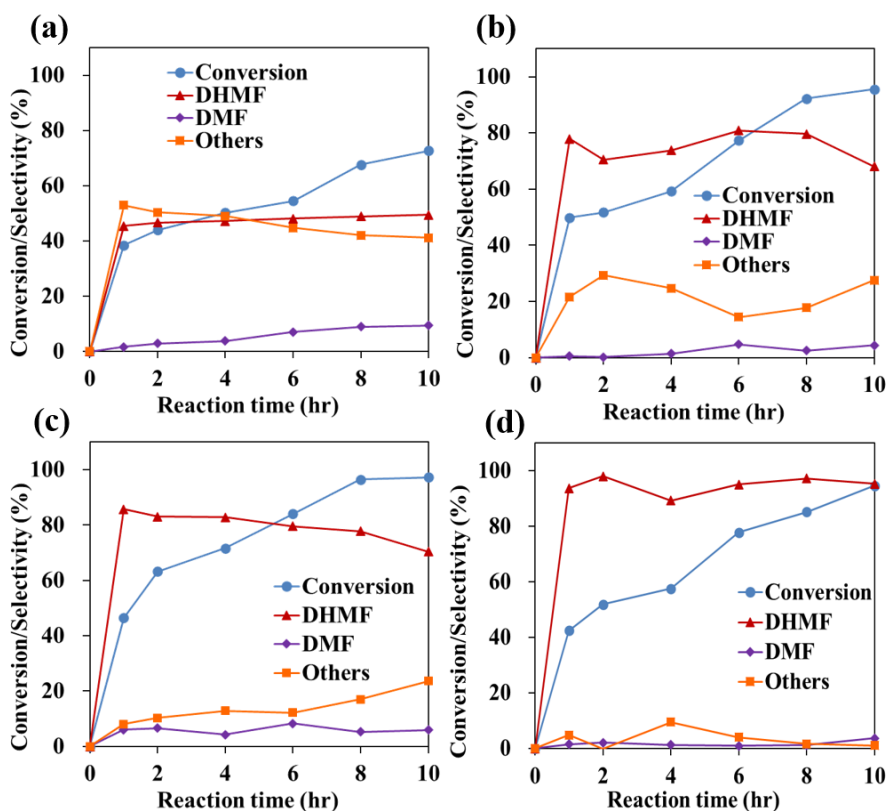
Figure S6. Conversion of HMF and selectivity to products versus reaction time for (a) Pt/CNTs-IM, (b) Pt/rGO-IM, (c) Pt/g-C_3N_4-IM, and (d) Pt/BC-IM catalysts. Reaction conditions: 0.5 g HMF, 0.1 g n-Tridecane, 40 mL 1-butanol, 50 mg catalyst, 160 °C, 10 bar H_2, and 500 rpm.
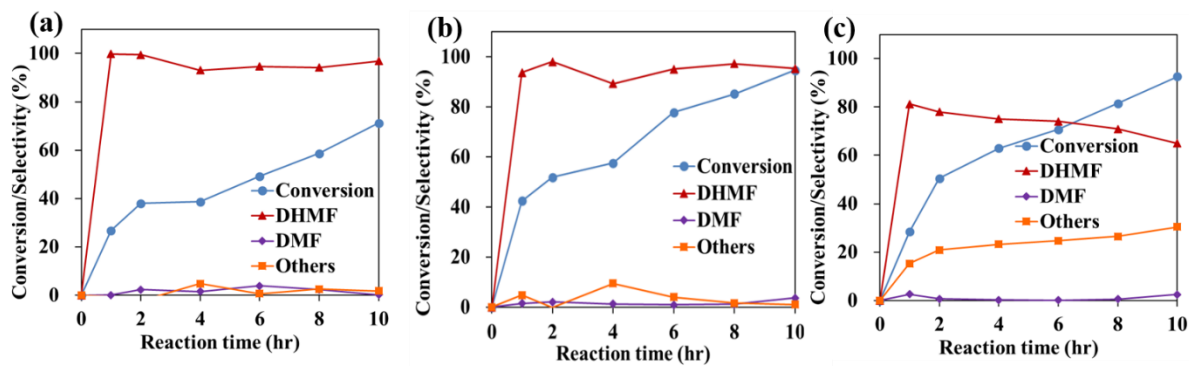
Figure S7. Effects of reaction temperature on the conversion of HMF and selectivity to products: (a) 140 °C, (b) 160 °C, and (c) 180 °C. Reaction conditions: 0.5 g HMF, 0.05 g n-Tridecane, 40 mL 1-butanol, 50 mg Pt/BC-IM catalyst, 10 bar H_2, and 500 rpm.
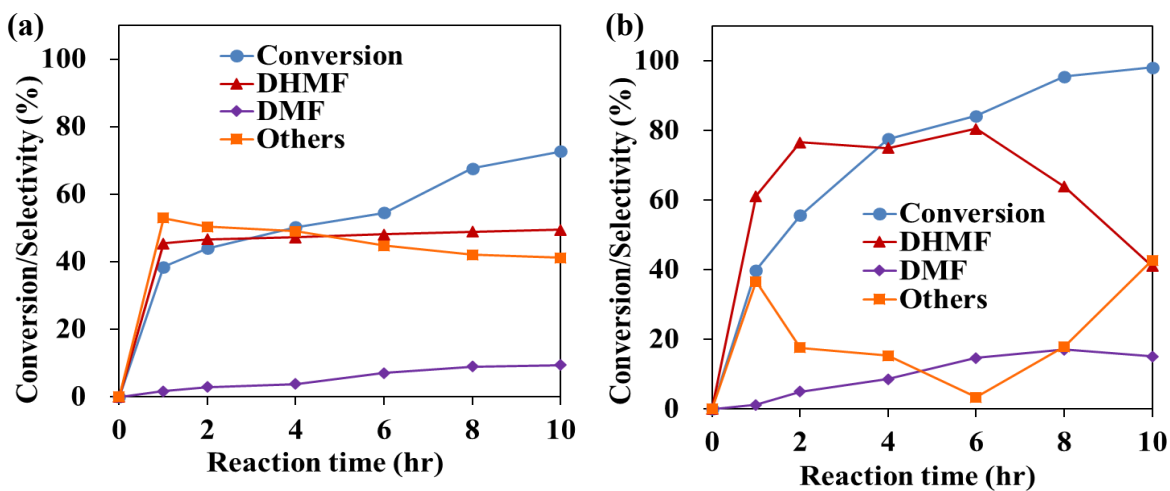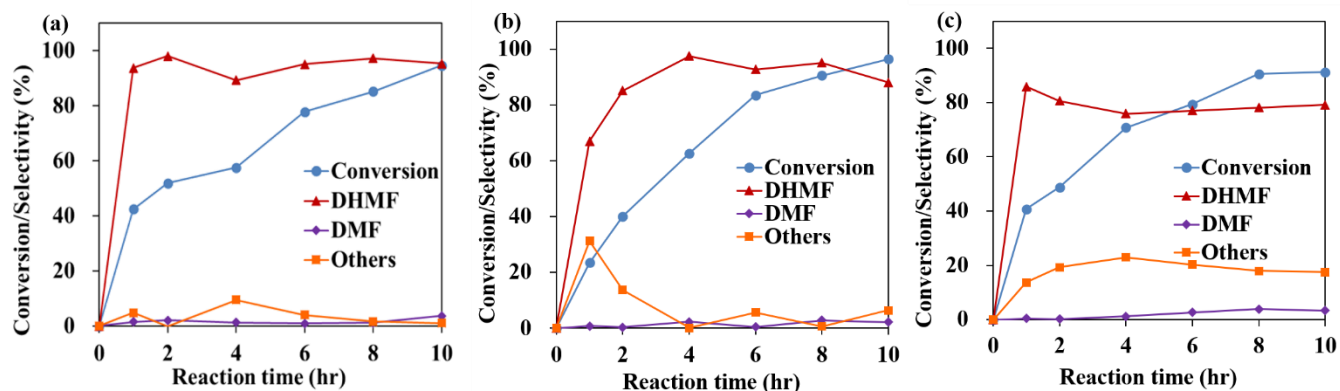

Figure S8. Effects of reaction temperature on the conversion of HMF and selectivity to products: (a) 160 °C and (b) 180 °C. Reaction conditions: 0.5 g HMF, 0.05 g n-Tridecane, 40 mL 1-butanol, 50 mg Pt/CNTs-IM catalyst, 10 bar H_2, and 500 rpm.

Figure S9. Effects of H$_2$ pressure on the conversion of HMF and selectivity to products: Pt/BC-IM catalyst at (a) 10 bar H$_2$, (b) 20 bar H$_2$ and (c) 30 bar H$_2$. Reaction conditions: 0.5 g HMF, 0.1 g n-Tridecane, 40 mL 1-butanol, 50 mg catalyst, 160 °C, and 500 rpm.
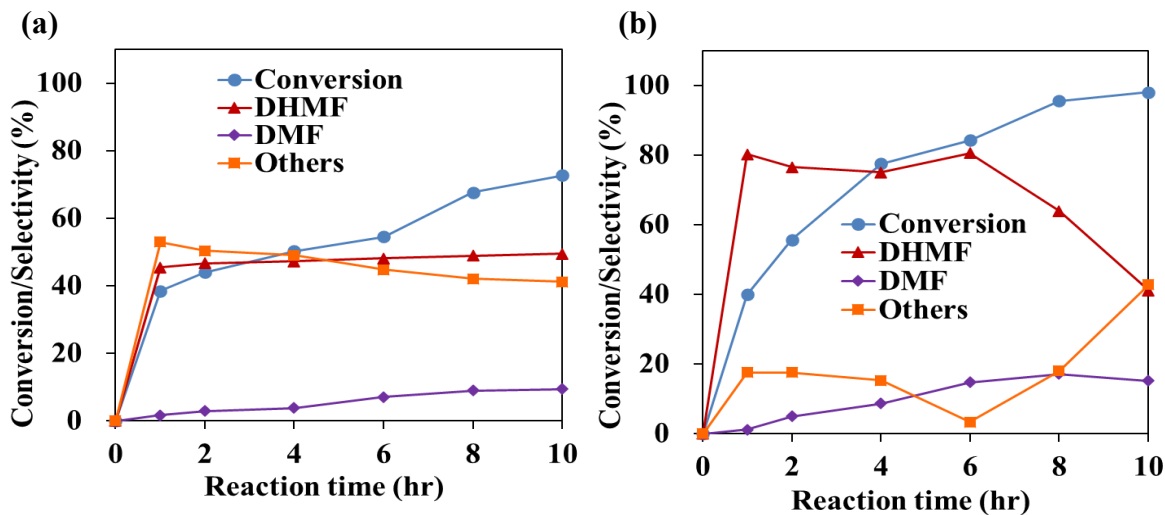

Figure S10. Effects of H$_2$ pressure on the conversion of HMF and selectivity to products: Pt/CNTs-IM catalyst at (a) 10 bar H$_2$ and (b) 30 bar H$_2$. Reaction conditions: 0.5 g HMF, 0.1 g n-Tridecane, 40 mL 1-butanol, 50 mg catalyst, 160 °C, and 500 rpm.
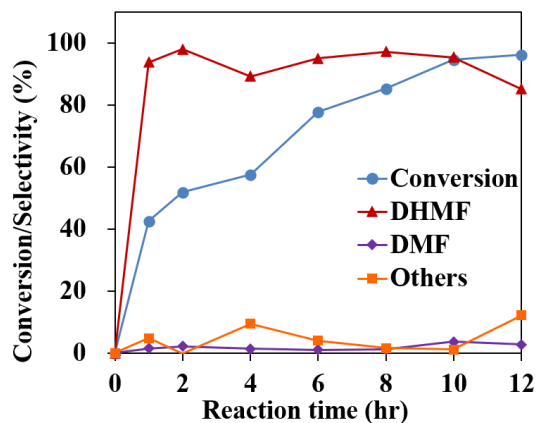
Figure S11. HMF conversion, selectivity to products over Pt/BC-IM catalyst. Reaction conditions: 0.5 g HMF, 0.05 g n-Tridecane, 40 mL 1-butanol, 50 mg catalyst, 160 °C, 10 bar H_2, and 500 rpm.
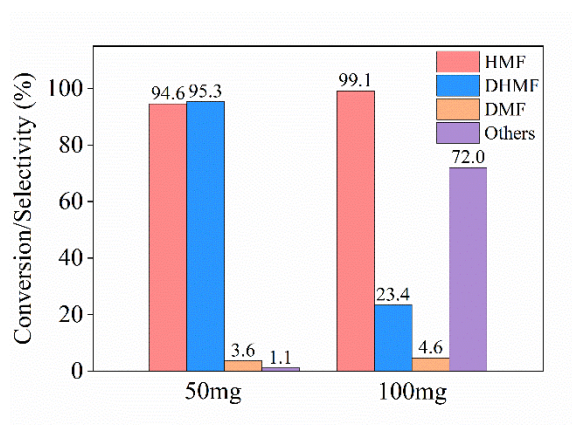

Figure S12. Effects of catalyst amount on the conversion of HMF and selectivity to products. Reaction conditions: 0.5 g HMF, 0.05 g n-Tridecane, 50/100 mg Pt/BC-IM catalyst, 40 mL 1-butanol, 10 bar H_2, 160°C, and 500 rpm.
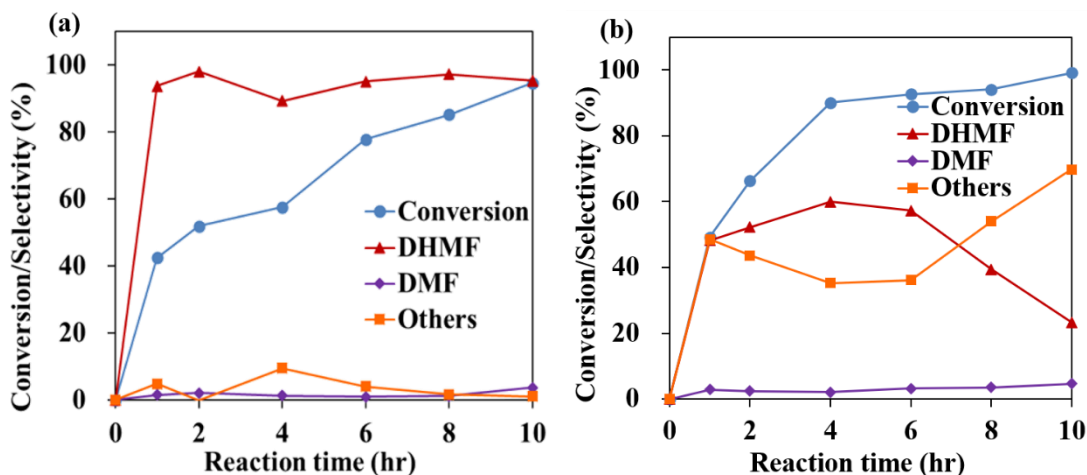
Figure S13. Conversion of HMF and selectivity to products versus reaction time: (a) 50 mg, and (b) 100 mg of Pt/BC-IM catalyst. Reaction conditions: 0.5 g HMF, 0.1 g n-Tridecane, 40 mL 1-butanol, 10 bar H_2, 160 °C, and 500 rpm.
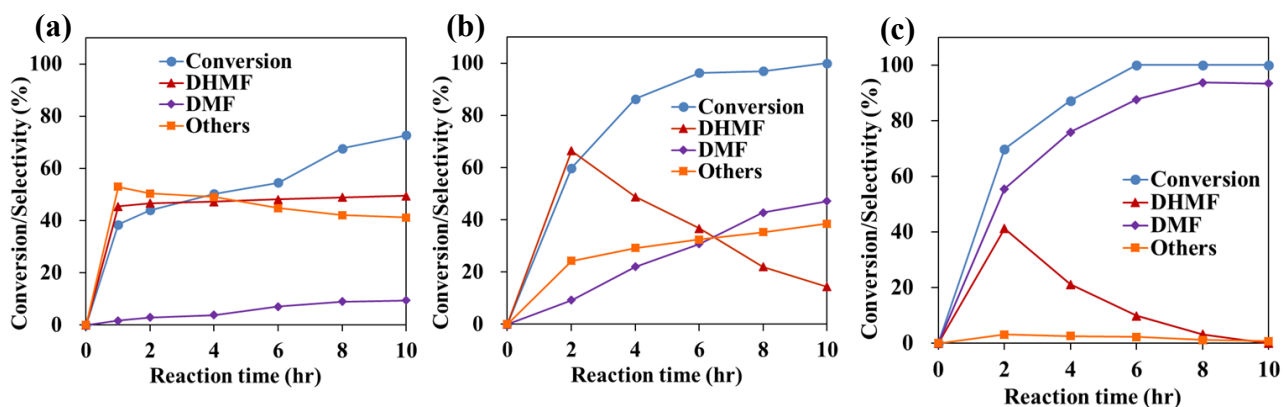

Figure S14. Conversion of HMF and selectivity to products versus reaction time for (a) Pt/CNTs-IM, (b) Pt/CNTs-ALD, and (c) PtNi/CNTs-ALD catalysts. Reaction conditions: 0.5 g HMF, 0.1 g n-Tridecane, 40 mL 1-butanol, 50 mg catalyst, 160 °C, 10 bar H_2, and 500 rpm.
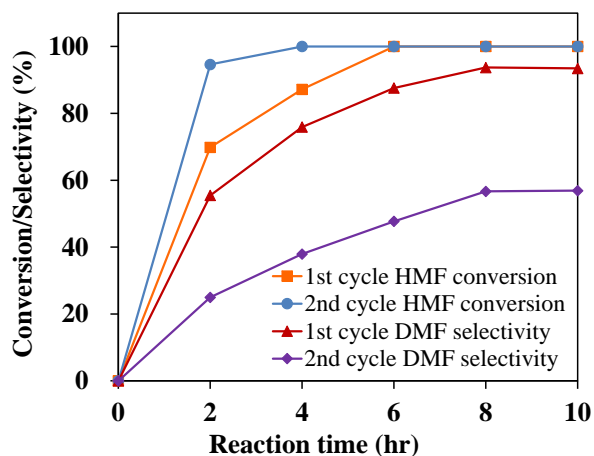
Figure S15. Conversion of HMF and selectivity to products in the cycling tests over PtNi/CNTs-ALD catalyst. Reaction conditions: 0.5 g HMF, 0.1 g n-Tridecane, 40 mL 1-butanol, 50 mg catalyst, 160 °C, 10 bar H_2, and 500 rpm.

References

[1]   Wang, Xiaofeng, Yufang He, Yuzi Liu, Jonghyun Park, and Xinhua Liang, Atomic layer deposited Pt-Co bimetallic catalysts for selective hydrogenation of α, β-unsaturated aldehydes to unsaturated alcohols. *Journal of Catalysis*, 2018. **366**: p. 61-69.

[2]   Wang, Xiaofeng, Yuzi Liu, and Xinhua Liang, Hydrogenolysis of 5-hydroxymethylfurfural to 2,5-dimethylfuran over supported Pt-Co bimetallic catalysts under mild conditions. *Green Chemistry*, 2018. **20**(12): p. 2894-2902.

[3]   Patel, Rajankumar L, Ying-Bing Jiang, and Xinhua Liang, Highly porous titania films coated on sub-micron particles with tunable thickness by molecular layer deposition in a fluidized bed reactor. *Ceramics International*, 2015. **41**(2): p. 2240-2246.